Investigation on the Modeling of Doubly-Fed Induction Generators for Wind Turbine

Yaakoub Diboune *, Djilali Kouchih
Automatic and Electrotechnics Department. Electrical Systems and Remote-Control Laboratory (LabSET). University of Blida 1 (USDB), Blida, Algeria
*yaakoubd479@gmail.com / diboune_yaakoub@univ-blida.dz

Abstract: Over recent decades, especially in the transmission network, the share of electricity produced by wind sources has significantly increased. In order to enhance the efficiency of the power system, it is crucial to have precise and comprehensive mathematical modeling of the generator for wind turbine systems. Typically, this generator is a doubly-fed induction generator, as its use of partial converters and induction machines makes it more economically successful compared to alternative technologies. In this paper, a novel approach has been developed for the modeling and analysis of doubly-fed induction generators. This thorough approach takes into account the derivation of the neutral voltage of the doubly-fed induction generator. This innovative approach has successfully extracted the fundamental harmonic of the stator currents and voltages with precision under normal operating conditions within a reasonable simulation time. It has been demonstrated that under normal operating conditions, a typical operation is achieved. It is characterized by a balanced stator voltage, current, flux, and fundamental harmonic through the stator variables, which correspond to the supply frequency. This fundamental harmonic has been suggested as a means of monitoring the generator during normal operating conditions. Mathematics modeling and simulation are conducted using MATLAB software. The validity and dependability of this method for analyzing and modeling doubly-fed induction generators are confirmed by the consistency and strong correlation between experimental and simulation results.

Keywords: Doubly-fed induction generators, Modeling, Simulation.

1. INTRODUCTION

Wind energy has emerged as a very promising candidate among renewable energy sources in recent years. Numerous wind turbine designs with diverse generator topologies have been developed to transform this plentiful energy into electrical power. The doubly-fed induction generator (DFIG) is the predominant generator type implemented in wind farms at present [1]-[5].

The main advantage of employing the DFIGs in wind turbines is their direct connection to the network through the three-phase stator windings, eliminating the need for supplementary converters. This topology has gained significant popularity for wind turbines operating at variable-speed [6]. The reason for this is mostly because the power electronic converter is required to manage just a small portion, ranging from 20% to 30%, of the overall power produced by the DFIG [7]. Thus, the losses occurring in the power electronic converter can be minimized.

The DFIG model can be represented in three reference frame: the stationary stator reference frame, the reference frame rotating at rotor speed, and the synchronous rotating reference frame. In order to streamline the controller design, the authors in [8, 9] included the synchronously rotating reference frame. This choice was made because all the currents and voltages represented under this reference frame will be of a direct current nature. In [10], the stator and rotor variables were defined in relation to their respective natural reference frames. The machine model developed in this reference frame is referred to as the "quadrature-phase slip-ring" model.

The modeling of the DFIG in a three-phase space (a-b-c reference) is excessively intricate due to the inclusion of coefficients that are dependent on θ, hence a function of time. To streamline these equations and derive a more accurate and straightforward model to manage the independence of these coefficients from the position θ, numerous approaches have been employed in the literature. To express the equations of the DFIG in a two-phase orthogonal reference frame in rotation (d-q reference), the authors in [11–17] used the Park transformer. This mathematical tool enables the derivation of a system of equations with constant coefficients. The relative components of the park are denoted as d (direct) and q (in quadrature). Also, Kaloi and al. present the dynamic model of the DFIG based wind turbine coupled to the grid system in the dq-

synchronous reference frame [18]. Another three-phase-two-phase transformation tools was also applied to modeling of DFIG, which is the Clarke transformer (α-β reference frame) [19]. In addition, Chico and Mazza used the Fortescue transformer for the modeling of DFIG [20]. Furthermore, Fan and al. used Hybrid modeling (dq-abc) of DFIGs for wind energy conversion systems [21].

Based on the state model approach [22], this paper presents a novel approach to model and assess the functioning of DFIGs under normal operating conditions, with the primary objective of ensuring the stability of stator currents and voltages. The spectrum analysis of stator currents and voltages can be employed as a robust method to monitor the performance of the system. This strategy offers various benefits. Firstly, it can be expanded to include the evaluation of DFIG performance under typical operating conditions. Furthermore, it offers exceptional precision and efficient simulation time [23]-[26]. The simulation results obtained from MATLAB and practical experiments provide evidence of the reliability, consistency and precision of this innovative approach for modeling and analyzing the behavior of DFIGs under normal operating conditions.

2. EQUATION OF DFIG

Equations for Stator Voltage

To illustrate this approach, a star-connected DFIG has been considered as illustrated by Fig.1. Which the stator connected with a balanced load R_l, while the stator voltages are unknown [27],[28].

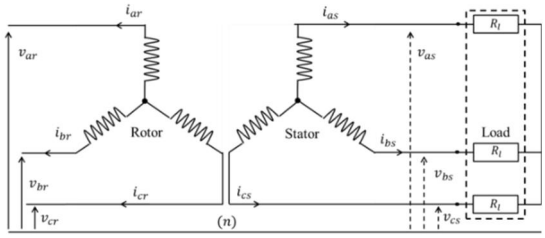

Fig. 1 Star connected DFIG.

The stator voltage is expressed by (1),

$$\frac{d[\Phi_{sh}]}{dt} = [R_s].[i_s] + [v_s] \quad (1)$$

With

$$[R_s] = \begin{bmatrix} r_{as} & 0 & 0 \\ 0 & r_{bs} & 0 \\ 0 & 0 & r_{cs} \end{bmatrix}$$

$[R_s]$ is the matrix of stator resistances.

Based on Ohm's law, we get (3).

$$[v_s] = -[R_l].[i_{sh}] \quad (3)$$

With

$$[R_l] = r_l \begin{bmatrix} 1 & 0 & 0 \\ 0 & 1 & 0 \\ 0 & 0 & 1 \end{bmatrix} \quad (4)$$

$[i_{sh}] = [i_{as} \;\; i_{bs} \;\; i_{cs}]^T$

i_{as} , i_{bs} and i_{cs} are the line currents.

$[R_l]$ is the matrix of the load resistances.

$[v_s] = [v_{as} \;\; v_{bs} \;\; v_{cs}]^T$

v_{as} , v_{bs} and v_{cs} are the phase voltages.

The stator flux vector is calculated using (5),

$$[\Phi_{sh}] = [T_h].[\Phi_s] \quad (5)$$

With

$$[T_h] = \begin{bmatrix} 1 & -1 & 0 \\ 0 & 1 & -1 \\ -1 & 0 & 1 \end{bmatrix} \quad (6)$$

$$[\Phi_s] = -[L_{ss}].[i_s] - [L_{sr}].[i_r] \quad (7)$$

$$[L_{ss}] = \begin{pmatrix} L_{ms} + L_{ls} & -\frac{L_{ms}}{2} & -\frac{L_{ms}}{2} \\ -\frac{L_{ms}}{2} & L_{ms} + L_{ls} & -\frac{L_{ms}}{2} \\ -\frac{L_{ms}}{2} & -\frac{L_{ms}}{2} & L_{ms} + L_{ls} \end{pmatrix} \quad (8)$$

$[\Phi_s] = [\Phi_{as} \;\; \Phi_{bs} \;\; \Phi_{cs}]^T$

$[L_{ss}]$ is the matrix of the stator inductances.

L_{ls} , L_{ms} are respectively the leakage and magnetizing inductance of the stator windings.

$[i_r]$ is the vector of the rotor currents.

We define the stator-rotor mutual inductances by:

$$[L_{sr}] = L_{sr}.\begin{pmatrix} \cos(\theta) & \cos\left(\theta + \frac{2\pi}{3}\right) & \cos\left(\theta - \frac{2\pi}{3}\right) \\ \cos\left(\theta - \frac{2\pi}{3}\right) & \cos(\theta) & \cos\left(\theta + \frac{2\pi}{3}\right) \\ \cos\left(\theta + \frac{2\pi}{3}\right) & \cos\left(\theta - \frac{2\pi}{3}\right) & \cos(\theta) \end{pmatrix}$$

Rotor Voltage Equations

The equation of rotor voltage is expressed by:

$$\frac{d[\Phi_r]}{dt} = [R_r].[i_r] + [v_r] \quad (10)$$

With

$$[v_r] = \begin{bmatrix} V_r \cos(\omega_r t) \\ V_r \cos(\omega_r t - \frac{2\pi}{3}) \\ V_r \cos(\omega_r t + \frac{2\pi}{3}) \end{bmatrix} \quad (11)$$

$$[R_r] = \begin{bmatrix} r_{ar} & 0 & 0 \\ 0 & r_{br} & 0 \\ 0 & 0 & r_{cr} \end{bmatrix} \quad (12)$$

$[v_r]$, $[R_r]$ are respectively the matrices of rotor voltages and resistances.

For the rotor flux equation, it is expressed using:

$$[\Phi_r] = -[L_{rs}].[i_s] - [L_{rr}].[i_r] \quad (13)$$

$$[L_{rs}] = [L_{sr}]^t \quad (14)$$

With

$$[L_{rr}] = \begin{pmatrix} L_{mr} + L_{lr} & -\frac{L_{mr}}{2} & -\frac{L_{mr}}{2} \\ -\frac{L_{mr}}{2} & L_{mr} + L_{lr} & -\frac{L_{mr}}{2} \\ -\frac{L_{mr}}{2} & -\frac{L_{mr}}{2} & L_{mr} + L_{lr} \end{pmatrix} \quad (15)$$

Where

$[L_{rr}]$ is the matrix of the rotor inductances;

L_{lr} , L_{mr} are respectively the leakage and magnetizing inductance of the rotor windings;

$[L_{rs}]$ is the rotor-stator mutual inductances;

Machine Current

Using (16) to (18), two independent components can be calculated i_{as} and i_{bs}, to obtain the stator currents defined by (16).

$$[i_{sh}] = [B_h][i_{abs}] \quad (16)$$

With

$$[B_h] = \begin{bmatrix} 1 & 0 \\ 0 & 1 \\ -1 & -1 \end{bmatrix} \quad (17)$$

$$[i_{abs}] = \begin{bmatrix} i_{as} \\ i_{bs} \end{bmatrix} \quad (18)$$

We define stator flux of two independent components by (19).

$$[\Phi_{abs}] = [A_h][\Phi_s] \quad (19)$$

With

$$[A_h] = \begin{bmatrix} 1 & -1 & 0 \\ 0 & 1 & -1 \end{bmatrix} \quad (20)$$

Using (19), the stator and rotor fluxes are expressed as illustrated by (21) to (25).

$$[\Phi_{abs}] = -[L_{sh}][i_{abs}] - [L_{srh}][i_r] \quad (21)$$

$$[\Phi_r] = -[L_{rsh}][i_{abs}] - [L_{rr}][i_r] \quad (22)$$

With

$$[L_{sh}] = [A_h][L_{ss}][B_h] \quad (23)$$

$$[L_{srh}] = [A_h][L_{sr}] \quad (24)$$

$$[L_{rsh}] = [L_{rs}][B_h] \quad (25)$$

Using (21) and (22), we get the equation of stator and rotor currents as illustrated by (26) and (27).

$$[i_{abs}] = [C_{sh}]([\Phi_{abs}] - [L_{srh}][L_{rr}]^{-1}[\Phi_r]) \quad (26)$$

$$[i_r] = [C_{rh}]([\Phi_r] - [L_{rsh}][L_{sh}]^{-1}[\Phi_{abs}]) \quad (27)$$

With

$$[C_{sh}] = -([L_{sh}] - [L_{srh}][L_{rr}]^{-1}[L_{rsh}])^{-1} \quad (28)$$

$$[C_{rh}] = -([L_{rr}] - [L_{rsh}][L_{sh}]^{-1}[L_{srh}])^{-1} \quad (29)$$

The State Model of DFIG

Using equations (1), (10), (26) and (27), the state model of DFIG is represented by,

$$\begin{cases} \frac{d[\Phi_{sh}]}{dt} = [R_s][B_h][C_{sh}]([\Phi_{abs}] - [L_{srh}][L_{rr}]^{-1}[\Phi_r]) + [v_{sh}] \\ \frac{d[\Phi_r]}{dt} = [R_r][C_{rh}]\left([\Phi_r] - [L_{rsf}][L_{sf}]^{-1}[\Phi_{abs}]\right) + [v_r] \\ \frac{d\Omega}{dt} = \frac{1}{J}(T_m - T_e - f_v\Omega) \end{cases}$$

Where J is the rotor and the connected load inertia, f_v is the viscose friction coefficient, Ω the mechanical angular speed, T_e the electromagnetic torque, and T_m the motorized torque.

We determine the electromagnetic torque by.

$$T_e = p[i_s]^t \frac{\partial[L_{sr}]}{\partial\theta}[i_r] \quad (31)$$

p, θ are respectively the poles pairs number and mechanical angle.

3. RESULTS AND DISCUSSION

Simulation results

The DFIG state model described above is simulated using MATLAB software. The DFIG of 220/380 V – 50 Hz – 4 kW, is operated at 3020 tr/mn, resulting in a 50 Hz fundamental frequency for the stator currents and voltages. The DFIG supplies a balanced load of R_l = 45 Ω. The stator voltages, currents and flux are shown in Figure 2(a), Fig.2(c) and Fig.2(e) respectively. Fig.2(b), Fig.2(d) and Figure 2(f) show the spectrum analysis of the stator voltage V_{as} , current I_{as} and flux Φ_{as} respectively. The electromagnetic torque and the rotor voltages are shown in Fig.3(a) and Fig.3(b) respectively.

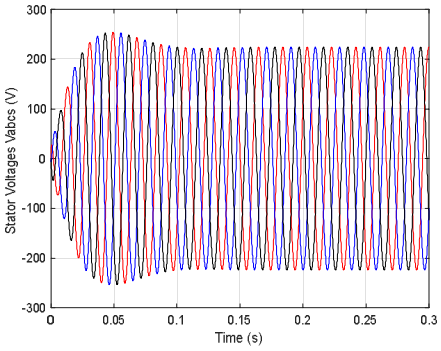

(a)

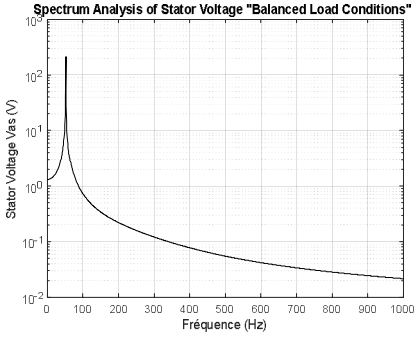

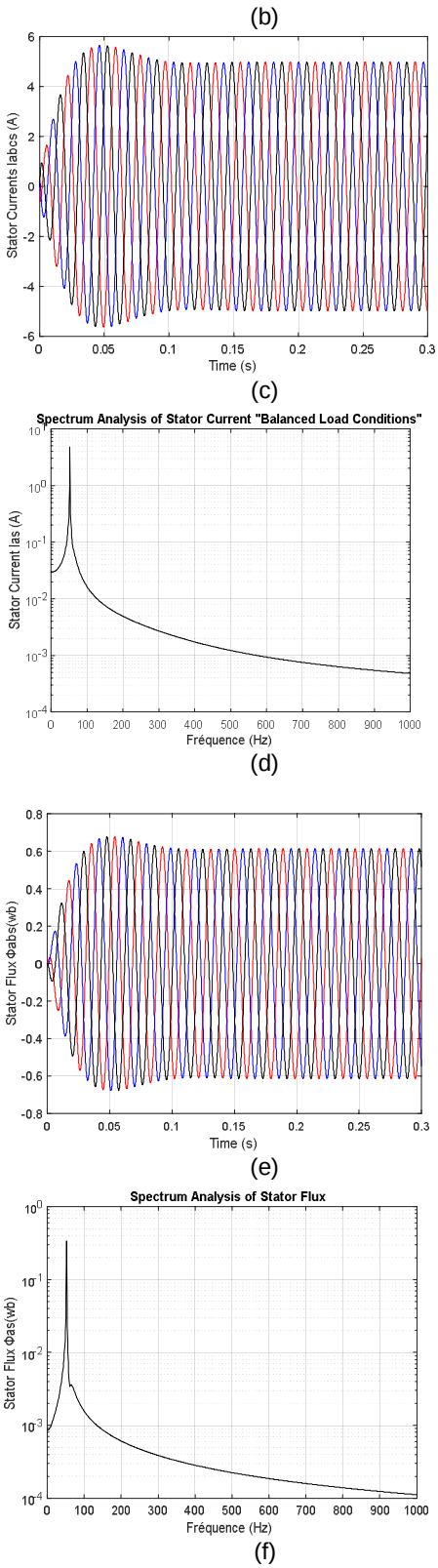

Fig. 2 Simulation results of DFIG: (a) stator voltagesV_{abcs}, (b) spectrum analysis of stator voltageV_{as}, (c) stator currentsI_{abcs}, (d) spectrum analysis of stator currentI_{as}, (e) stator fluxΦ_{abcs}, and (f) spectrum analysis of stator fluxΦ_{as}.

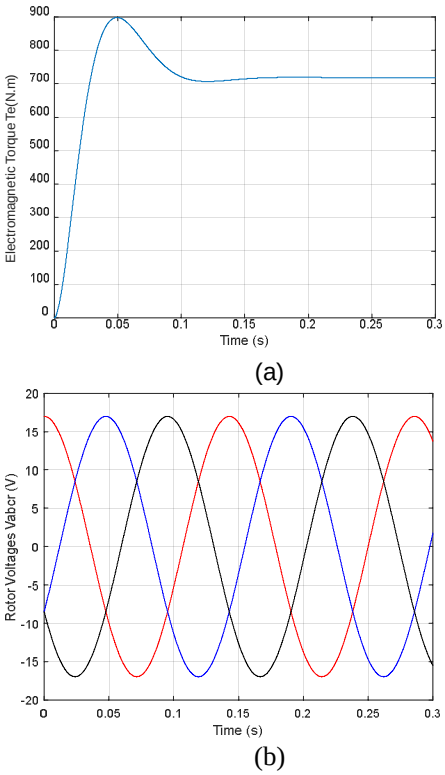

Fig. 3 Simulation results of DFIG: (a) Electromagnetic torque$\boldsymbol{T_e}$, and (b) Rotor voltages$\boldsymbol{V_{abcr}}$.

The simulation results obtained show the importance of the stator currents during the start-up; after a time equal to about 0.1 s, they stabilize and take their sinusoidal forms with a frequency of 50 Hz for the currents, the fluxes and the stator voltages. It is also noted that during the dynamic regime, the electromagnetic torque is positive, reaching at the start a maximum value of almost 900 N.m, as shown in Fig.3(a). In addition, we observe the stability of the rotor voltages as shown in Fig.3(b). A fundamental harmonic is detected through the stator voltages, currents and flux spectrum analysis, which corresponds to the supply frequency (50Hz) as shown in Fig.2(b), Fig.2(d) and 2(f), respectively. This balanced operation ensures optimal performance of the DFIG.

Experimental results

An experiment was conducted on a DFIG with 220/380 V - 50 Hz and a power of 4 kW, in order to verify the validity of the theoretical analysis. The DFIG is mechanically coupled to a direct motor rotating at 3020 tr/mn and generating a 50 Hz fundamental frequency for the stator voltages. The DFIG starts with no load, then introduces a balanced load of R_l = 45 Ω. Shunt resistors are used for measuring the stator currents. The stator and rotor voltages are shown in Fig.4(a), and

Fig.4(b) respectively. Fig.4(c), and Fig.4(d) illustrate the spectrum analysis of the stator and rotor voltages (V_{as}, V_{ar}) respectively.

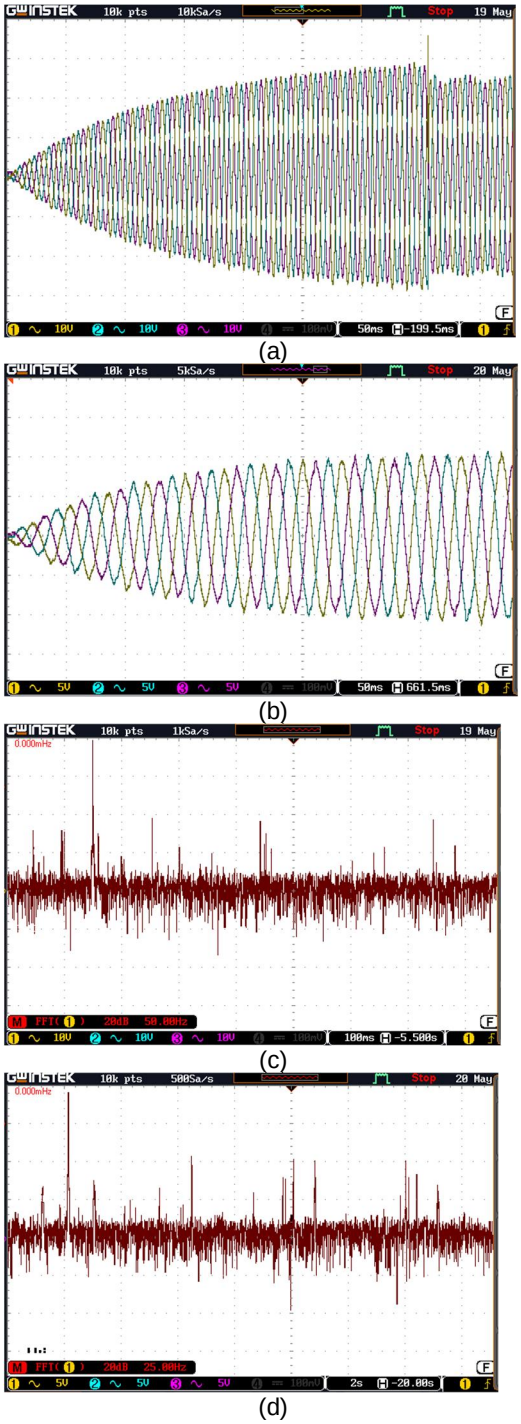

Fig. 4 Experimental results of DFIG: (a) stator voltages$\boldsymbol{V_{abcs}}$, (b) rotor voltages$\boldsymbol{V_{abcr}}$, (c) stator voltage spectrum analysis$\boldsymbol{V_{as}}$, and (d) rotor voltage spectrum analysis$\boldsymbol{V_{ar}}$.

As illustrated by Fig.4(a) and 4(b), experimental results during normal operating conditions, show balanced stator and rotor voltages. We observe the presence of certain harmonics in the spectrum analysis of the stator and rotor voltages, such as 150 Hz, 250 Hz, 350 Hz, although their values are small. This is attributed to the non-ideal characteristics of the power supply, as shown in Fig.4(c) and 4(d). Therefore, maintaining balanced stator and rotor voltages is crucial for ensuring the optimal performance, longevity, and safe operation of the DFIG. Experimental results that correspond with simulation results confirm the balance and stability of the stator and rotor variables during normal operating conditions.

4. CONCLUSION

Theoretical and experimental research has been conducted to analyze the Doubly-Fed Induction Generator (DFIG) under normal operating conditions and extract key electromagnetic characteristics such as stator voltages, currents, and flux. Normal operation is defined by balanced stator voltages and currents, with the presence of the fundamental harmonic at 50 Hz in the stator variables. To monitor this normal operation, it is proposed to analyze the frequency of stator voltages and currents. This method provides accurate results within a reasonable simulation time. Future work could focus on refining this approach to better distinguish normal operating conditions from potential deviations.

References

[1] H. Benbouheni , “Application of DPC and DPC-GA to the dual-rotor wind turbine system with DFIG”, International Journal of Robotics and Automation, vol.10, no .3, pp.224-234, Sep. 2021, doi: 10.11591/ijra.v10.i3.pp224-234.

[2] R. Mahroug, M. Matallah, and S. Abudura, “Modeling of wind turbine based on dual DFIG generators,” International Journal of Power Electronics and Drive Systems, vol. 13, no. 2, pp. 1170–1185, Mar.2022, doi: 10.11591/ijpeds.v13.i2.pp1170-1185.

[3] Y.M. Alsmadi, et al.”Detailed investigation and performance improvement of the dynamic behavior of grid-connected DFIG-based wind turbines under LVRT conditions”.IEEE Trans. Ind. Appl., 54 (5) (2018), pp. 4795-4812.

[4] M. A. Soomro, Z. A. Memon, M. Kumar, M. H. Baloch,“Wind energy integration: Dynamic modeling and control of DFIG based on super twisting fractional order terminal sliding mode controller”.Energy Reports,Volume 7,2021,Pages 6031-6043, doi:10.1016/j.egyr.2021.09.022.

[5] G.S. Kaloi, J. Wang, M.H. Baloch,”Active and reactive power control of the doubly fed induction generator based on wind energy conversion system”. Energy Rep., 2 (2016), pp. 194-200.

[6] B. C. Babu and K. B. Mohanty, "Doubly-fed induction generator for variable speed wind energy conversion systerns-modeling &

simulation," het. J. Comput. Electr. Eng., vol. 2, no. 1, pp. 141-147, 2010, doi: 10.7763/IJCEE.2010.V2.127

[7] S.M.Alwash, O.Q.J. Al-Thahab, S.F. Alwash, “Modeling and control strategies for DFIG in wind turbines: A comparative analysis of SPWM, THIPWM, and SVPWM techniques”. Journal Européen des Systèmes Automatisés, Vol. 56, No. 6, pp. 963-972. (2023). doi :10.18280/jesa.560607.

[8] J.B. Ekanayake, L. Holdsworth, X. Wu, N. Jenkins, Dynamic modeling of doubly fed induction generator wind turbines. IEEE Trans. Energy Convers. 18, 803–809 (2003)

[9] I. Erlich, J. Kretschmann, J. Fortmann, S. Mueller-Engelhardt, H. Wrede, Modeling of wind turbines based on doubly-fed induction generators for power system stability studies. IEEE Trans Energy Convers. 22, 909–919 (2007)

[10] A.Tapia, G. Tapia, J.X. Ostolaza, J.R. Saenz, Modeling and control of a wind turbine driven doubly fed induction generator. IEEE Trans. Energy Convers. 18, 194–204 (2003)

[11] I. Khan and al. “Dynamic Modeling and Robust Controllers Design for Doubly Fed Induction Generator-Based Wind Turbines under Unbalanced Grid Fault Conditions”. Energies 2019, 12(3), 454, doi: 10.3390/en12030454.

[12] N. k. Mishra, Z. Husain, A. Iqbal:“Modeling and analysis of novel six-phase DFIG through asymmetrical winding structure for disperse generation”. WILEY International Transactions on Electrical Energy Systems, 30(12), DOI:10.1002/2050-7038.12649.

[13] B. Hamane, M. L. Doumbia, M. Bouhamida and M. Benghanem, "Control of wind turbine based on DFIG using Fuzzy-PI and Sliding Mode controllers," 2014 Ninth International Conference on Ecological Vehicles and Renewable Energies (EVER), Monte-Carlo, Monaco, 2014, pp. 1-8, doi: 10.1109/EVER.2014.6844060.

[14] L. Amira, B. Tahar and M. Abdelkrim, "Sliding Mode Control of Doubly-fed Induction Generator in Wind Energy Conversion System," 2020 8th International Conference on Smart Grid (icSmartGrid), Paris, France, 2020, pp. 96-100, doi: 10.1109/icSmartGrid49881.2020.9144778.

[15] D. R. Karthik, Narayan S. Manjarekar, Shashidhara Mecha Kotian, Computation of steady-state operating conditions of a DFIG-based wind energy conversion system considering losses, Electrical Engineering, 10.1007/s00202-023-01766-x, 105, 3, (1825-1838), (2023). 406.

[16] Belachew Desalegn, Desta Gebeyehu, Bimrew Tamrat, Smoothing electric power production with DFIG-based wind energy conversion technology by employing hybrid controller model, Energy Reports, 10.1016/j.egyr.2023.06.004, 10, (38-60), (2023).

[17] A. Khan, H. A. Khalid, M. Uzair Khalid and M. Khan, "Dynamic Modeling, Operations, and Steady-State Analysis of DFIG based Nordex S77 Wind Turbine," 2022 International Conference on Electrical Engineering and Sustainable Technologies (ICEEST), Lahore, Pakistan, 2022, pp. 1-6, doi: 10.1109/ICEEST56292.2022.10077858.

[18] G. S. Kaloi, J.Wang, M. Baloch:” Dynamic Modeling and Control of DFIG for Wind Energy Conversion System Using Feedback Linearization”. Journal of Electrical Engineering and Technology, vol.11, no.5, pp.1137-1146, Sep.2016, doi:10.5370/JEET.2016.11.5.1137.

[19] J.P. Barton, D.G., “Infield, Energy storage and its use with intermittent renewable energy,” IEEE Transactions on Energy Conversion, vol. 19, no. 2, pp. 441-448, 2004.

[20] G. Chicco, A. Mazza:”100 years of symmetrical components”. Energies, 2019,12(3), 450. Doi:10.3390/en12030450.

[21] L. Fan, Z. Miao, S. Yuvarajan, R. Kavasseri“Hybrid modeling of DFIGs for wind energy conversion systems”. Simulation Modelling Practice and Theory, Volume 18, Issue 7, August 2010, Pages 1032-1045, doi: 10.1016/j.simpat.2010.04.002.

[22] D. Kouchih and R. Hachelaf, “Theoretical and Experimental Analysis of the Squirrel Cage Induction Generators Operating under Unbalanced Conditions” , Research Square, vol. 1, no. 1,pp. 1–12, Dec. 2022, doi: 10.21203/rs.3.rs-2347428/v1.

[23] S. Abdi, E. Abdi, and R. McMahon,”Experimental and Finite Element Studies of a 250 kw Brushless Doubly Fed Induction Generator”, IET Journal of Engineering, vol. 2019, no. 12, pp. 8489-8495, Nov. 2019, doi: 10.1049/joe.2018.5272.

[24] J. Cheng, H. Z. Ma, S. Song, and Z. Xie, “Stator Inter-turn Fault Analysis in Doubly-Fed Induction Generators using rotor current based on Finite Element Analysis”, in IEEE Int. Conf. on Prog. in Info. and Comp. (PIC), Suzhou, China, Dec. 2018, pp.414-419, doi: 10.1109/pic.2018.8706293.

[25] Y. Chen et al.,”FEM simulation and Analysis on Stator Winding Inter-turn Fault in DFIG”, In IEEE 11th Int. Conf. on the Prop. and App. Of Diel. Mat.(ICPADM), Sydney, NSW, Australia, Jul. 2015, pp. 244-247, doi: 10.1109/icpadm.2015.7295254.

[26] H. Mellah, S. Arslan, H. Sahraoui, K. E. Hemsas, and K. Saoudi, “The Effect of Stator Inter-turn Short-Circuit Fault on DFIG Performance Using FEM”, Eng., Tech. and Appl. Science Research, vol. 12, no. 3, pp. 8688-8693, May. 2022, doi: 10.48084/etasr.4923.

[27] D. Kouchih, N. Boumalha, M. Tadjine, and M.S. Boucherit, “New approach for the modeling of induction machines operating under unbalanced power system”, International Transactions on Electrical Energy Systems, vol. 26, no. 9, pp. 1832-1846, Jan. 2016, doi: 10.1002/etep.2171.

[28] Y. Diboune, R. Hachelaf and D. Kouchih, “Theoretical and experimental analysis of unbalanced doubly fed induction generators”, International Journal of Robotics and Automation IJRA, vol. 13, no. 4, pp. 476-484, Dec. 2024, doi: 10.11591/ijra.v13i4.pp476-484.